Flow and Fracture of Alloys in the Fusion Environment

W.G. Wolfer and R.H. Jones

August 1981

UWFDM-429

Paper presented at Second Topical Mtg. on Fusion Reactor Materials, August 9-12, 1981, Seattle, WA; J. Nucl. Matls. 103 & 104, 1305-1314 (1981).

FUSION TECHNOLOGY INSTITUTE

UNIVERSITY OF WISCONSIN

MADISON WISCONSIN

Flow and Fracture of Alloys in the Fusion Environment

W.G. Wolfer and R.H. Jones

Fusion Technology Institute
University of Wisconsin
1500 Engineering Drive
Madison, WI 53706

http://fti.neep.wisc.edu

August 1981

UWFDM-429

Paper presented at Second Topical Mtg. on Fusion Reactor Materials, August 9-12, 1981, Seattle, WA; J. Nucl. Matls. 103 & 104, 1305-1314 (1981).

Flow and Fracture of Alloys in the Fusion Environment

W.G. Wolfer
R.H. Jones*

Fusion Engineering Program
Nuclear Engineering Department
University of Wisconsin
Madison WI 53706

August 1981

UWFDM-429

*Battelle Memorial Institute, Pacific Northwest Laboratories, Richland WA 99352.

FLOW AND FRACTURE OF ALLOYS IN THE FUSION ENVIRONMENT

W. G. Wolfer
Fusion Engineering Program, Department of Nuclear Engineering
University of Wisconsin, Madison, WI 53706, USA

R.H. Jones
Battelle Memorial Institute, Pacific Northwest Laboratories
Richland, WA 99352, USA

The present paper examines both ductile and brittle fracture models of steels and assesses the impact of the fusion reactor environment on the fracture processes. In particular, the connections between plastic flow properties and fracture modes are reviewed for both ductile and brittle crack propagation. Highly radiation-hardened materials exhibit extreme flow localization resulting in channel fracture. Physical models for this phenomon are developed and an estimate for the associated fracture toughness is given. The impact of radiation-hardening and ductility loss on fatigue crack growth is examined. Next, models describing the chemical effects on fatigue and fracture are briefly discussed. Finally, fracture design criteria are proposed for first wall structures in fusion reactors.

1. INTRODUCTION

It is by now well established that the economic feasibility of fusion reactors will depend to a large degree on the lifetime of the first wall. The ultimate failure mode of a first wall depends in a complicated and synergistic manner on many factors which are indicated in Fig. 1 together with the logical interconnections among them. Of central importance to the topic of the present paper are the following connections. Exposure to elevated temperatures, neutron flux, and to corrosive agents from the coolant and the plasma, will result in changes of the mechanical properties. These changes together with the stresses imposed lead to a damage accumulation in the structural materials which may eventually result in failure. The most prevalent failure modes for tokamak reactors are fatigue crack growth, embrittlement, and finally plastic flow or brittle fracture [1].

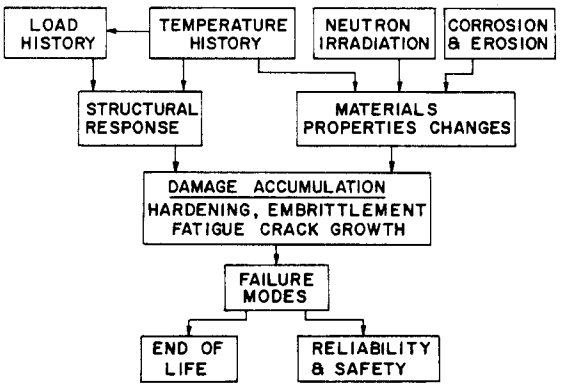

Fig. 1. Methodology for failure analysis of the first wall.

Although plastic flow and fracture are processes involved only in the terminal phase of the lifetime for the first wall, they are nevertheless of interest at all stages of the damage accumulation, because they also characterize the latter.

The ductility of structural materials and their mode of fracture can change dramatically with neutron radiation damage. For example, radiation-induced hardening reduces the difference between ultimate and yield stress in certain materials to such an extent that plastic flow becomes highly localized. Fracture changes then from ductile rupture to shear decohesion with a dramatic reduction in ductility. This example demonstrates that there exists a close interrelationship between the modes of plastic flow and fracture. Hence, there exists for example the possibility, to assess the fracture toughness of irradiated materials utilizing tensile properties which can be obtained on much smaller samples. In addition, tensile and plastic flow properties can be related more directly to the microstructure than fracture toughness or fatigue crack growth data.

The mode of plastic deformation in crack propagation also determines the mode and severity of a potential failure of the first wall. Depending on the value of the fracture toughness, yield strength, and wall thickness at the time of failure, it can either be a small leak before catastrophic and large-scale fracture or the latter. In terms of maintenance, safety, and repair, the mode of failure can make a dramatic difference. In view of these issues, the purpose of this paper is to review and to examine the deformation processes involved in a potential failure of a first wall, and to indicate

how radiation and environmental effects will most likely influence these processes. We shall assume that the first wall is operated at a sufficiently low temperature that intergranular failure is avoided. This implies, in the case of a stainless steel wall, that the operating temperature is below about 500°C.

In section 2, we review models of fracture toughness aimed at relating this important property to tensile properties of alloys which exhibit homogeneous plastic deformation. Since radiation hardening may lead to flow localization, we discuss separately in section 3 the status of our understanding for channel deformation and fracture. The connection between fracture toughness and fatigue crack growth is briefly discussed in section 4. Section 5 is devoted to a discussion of chemical effects of fracture and fatigue. Finally, fracture design criteria are explored in section 6.

2. FRACTURE TOUGHNESS AND TENSILE PROPERTIES FOR HOMOGENEOUS PLASTICITY

Materials which exhibit substantial work-hardening deform plastically in a more or less uniform manner in simple tensile tests. When one considers then the plastic deformation ahead of a crack tip, it is reasonable to assume that plastic flow is governed by the same deformation law as obtained from a homogeneous deformation experiment. The nonuniform deformation in the plastic zone of the crack tip is merely due to the nonuniform stress distribution. Both distributions for stress and plastic strain can therefore be obtained with the macroscopic deformation law, e.g., with $\sigma = \sigma_0 \varepsilon^n$. Here σ_0 is a constant with the dimensions of stress, ε is the plastic strain, and n is the strain hardening exponent. The following models for the fracture toughness make use of such a plastic stress-strain analysis at the crack tip and combine it with various failure criteria.

2.1 The Hahn-Rosenfield (HR) Model

The condition for crack advancement in the HR model [2] is that the strain in the plastic zone ahead of the crack tip must exceed a critical value ε^*. The plastic deformation field is modeled according to the modified Bilby-Swinden theory. Whereas in the original model of Bilby and Swinden [3] the plastic deformation consists of two slip-lines emanating from the crack tip under an angle of 45° to the crack plane (as shown in Fig. 2), the modified plastic field has two plastic zones of finite width ℓ with a mean inclination of 75°. The width ℓ is dependent on the strain hardening exponent n.

Ductile failure ahead of the crack involves nucleation, growth, and link-up of cavities formed at precipitates. The critical strain ε^* for link-up is assumed to be 1/3 of the uniaxial fracture strain ε_f for plane strain. The fracture toughness is then given by

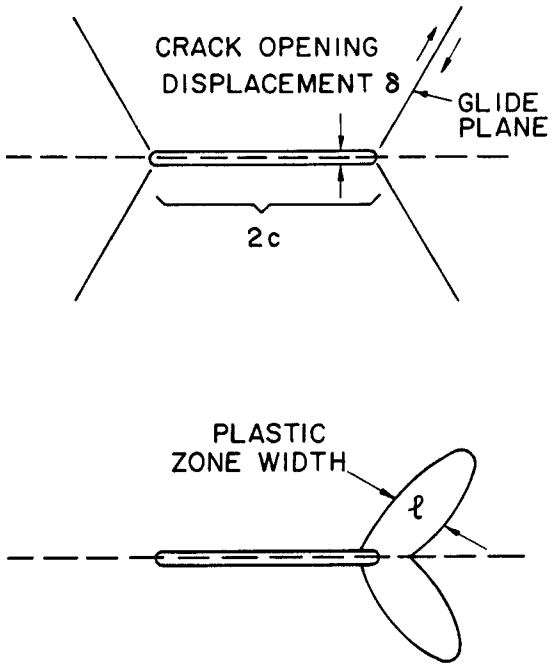

Fig. 2. Crack tip deformation models.

$$K_{Ic} \cong \left[\frac{2}{3} E \sigma_Y \ell \varepsilon_f\right]^{1/2} , \qquad (1)$$

where E is the Young's modulus and σ_Y the yield stress.

Hahn and Rosenfield compared Eq. (1) to measured data for K_{Ic}, σ_Y, and ε_f, and found that the plastic zone width ℓ is empirically given by

$$\ell(n) = 0.0013 + 2.54\ n^2 \quad (cm) \ . \qquad (2)$$

If not available, the strain hardening exponent n can be approximated by the ultimate tensile strain ε_{UTS}, so that $\ell \cong 2.54\ \varepsilon_{UTS}^2$.

The application of the HR model to the tensile data for HFIR-irradiated 20% CW type 316 stainless steel [4] gives values for the fracture toughness shown as open symbols in Fig. 3. It is seen that the fracture toughness decreases with dose as a result of ductility loss. It appears, however, that the predicted fracture toughness for the unirradiated samples is too low, perhaps by a factor of two [5].

2.2 The Krafft (K) Model

In the fracture model of Krafft [6], crack propagation is assumed to occur when the plastic strain exceeds a critical value over a distance d^* of a so-called process zone ahead of the

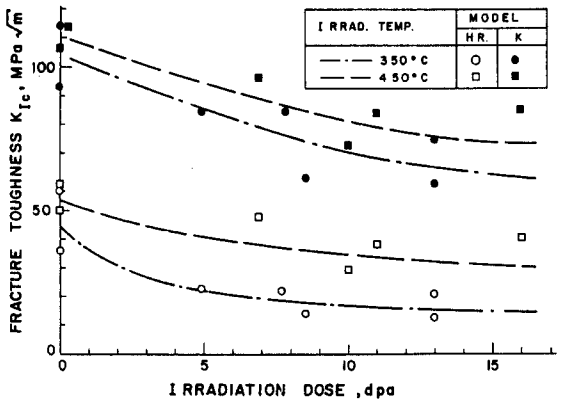

Fig. 3. Fracture toughness predictions based on tensile data for HFIR irradiated 20% CW 316 SS.

crack tip. The strain distribution in this process zone is given by

$$\varepsilon/\varepsilon_Y = \left[\frac{(1 - 2\nu)K^2}{(1 + n)\pi r\sigma_Y^2}\right]^{(1/(1+n))} , \qquad (3)$$

where ν is the Poisson's ratio, ε_Y is the plastic strain at the yield point, K is the stress intensity factor, and r is the distance from the crack tip. Setting $\varepsilon = \varepsilon_f$ and $r = d^*$ in Eq. (3) gives the fracture toughness as

$$K_{Ic} = \frac{\sigma_Y}{(1-2\nu)}\left[\pi(1+n)d^*(\varepsilon_f E/\sigma_Y)^{(1+n)}\right]^{1/2} . \qquad (4)$$

The process zone diameter, d^*, is now assumed to be equal to the dimple spacing on a fracture surface. When no fractographic information is available, d^* may be approximated by the grain size or the average planar distance between inclusions.

Using again the approximation $n \cong \varepsilon_{UTS}$, $d^* = 25$ μm, and the tensile data of the HFIR-irradiated samples [4], the K-model gives fracture toughness values as shown by the solid symbols in Fig. 3. The K_{Ic} values for the unirradiated samples are in better agreement with measured values [5]. Furthermore, the K-model predicts values which are larger by a factor of two than the values obtained with the HR model. It is also interesting to note that the K-model shows a weak dependence of K_{Ic} on the irradiation temperature, whereas a strong dependence is obtained with the HR model.

Although both models give similar reductions of the fracture toughness with increasing dose, the absolute values for K_{Ic} at any given dose can only be predicted within a factor of 2 or 3. This factor appears to be the typical uncertainty for most fracture toughness models applicable to ductile rupture, and it originates from the ill-defined microstructural parameter which characterizes the plastic or process zone.

A better definition of the relevant microstructural features involved in the ductile void formation, as well as a calibration of the various models with actual K_{Ic} data for irradiated materials appears to be the most fruitful way to improve the predictive capability of present models for ductile fracture toughness.

It must be emphasized, however, that although fracture models provide important empirical guidelines for alloy development, they are no substitute for actual fracture mechanics data needed ultimately for fusion reactor design.

2.3 The Ritchie-Knott-Rice (RKR) Model

This model was developed by Ritchie, Knott, and Rice [7] for bcc alloys to explain the ductile to brittle transition with decreasing temperature. More recently, Parks [8] and Ritchie et al. [9] have extended the model to irradiated nuclear pressure vessel steels. The model consists of two different parts, one applicable to the lower, and the other to the upper shelf fracture toughness.

For brittle fracture below the ductile to brittle transition temperature (DBTT), failure is assumed to occur when the local stress σ in front of the crack tip exceeds a critical value σ^* over a characteristic length λ^*, at which point slip-initiated cleavage takes place. The two parameters, σ^* and λ^*, are considered to be basic materials parameters independent of temperature and dislocation density. It is also assumed that σ^* and λ^* are independent of the radiation damage.

The stress distribution within the plastic zone is taken to be that for "small-scale yielding", and it is given by [10]

$$\sigma/\sigma_Y = f(N)\left[\frac{(1 - \nu^2)K^2}{I\sigma_Y\varepsilon_Y Er}\right]^{(1/(1+N))} . \qquad (5)$$

Here, the plastic deformation law is written as

$$\varepsilon/\varepsilon_Y = (\sigma/\sigma_Y)^N , \qquad (6)$$

so that $N = 1/n$, and σ_Y and ε_Y are the stress and strain at the yield point, respectively. I is a parameter weakly dependent on N, and f(N) is an angular function of order one.

The above mentioned fracture condition implies that Eq. (5) yields the fracture toughness when $\sigma = \sigma^*$ at $r = d^*$. Hence, the lower shelf fracture toughness is given by

$$K_{Ic} = [\lambda^* I/(1-\nu^2)]^{1/2}(\sigma^*/f)^{(N+1)/2}\sigma_Y^{(N-1)/2}. \quad (7)$$

The slip-initiated cleavage is thought to originate at grain boundary carbides, so that λ^* is about two to four grain diameters.

The critical fracture stress σ^* can be determined experimentally by fracturing V-notched specimens at sufficiently low temperatures, so that failure occurs without gross yielding when the maximum stress at the notch root becomes equal to σ^*.

Ritchie et al. [9] have shown that Eq. (7) does indeed provide an excellent correlation between measured tensile data and the lower shelf fracture toughness of irradiated nuclear pressure vessel steels. σ^* and λ^* are obtained from unirradiated samples and subsequently used also for irradiated samples. Considering the low irradiation doses involved in these experiments, one would not expect any changes of the parameters σ^* and λ^*, except of course the increase of the yield strength σ_Y and the concomitant shift in the DBTT.

However, radiation-induced segregation and precipitation are known to occur during long neutron exposures, resulting in substantial changes of the microstructure and the alloy matrix composition. Furthermore, the concentrations of minor alloy elements, which play a significant role in the mechanical strength of structural alloys, can be changed markedly by nuclear transmutations. As a result, it must be expected that σ^* and λ^* will change in a fusion reactor environment.

For temperatures above the DBTT, where $\sigma_Y < \sigma^*$, crack propagation occurs by ductile tearing rather than by slip-initiated cleavage.

Ritchie et al. [9] assume for this fracture process that the plastic strain ahead of the crack tip must exceed a critical value ε_f^* over a characteristic length ℓ^*. Although this fracture criterion is similar to those used in the HR and K models, their derivation of the ductile fracture toughness entails different arguments. First, the plastic strain distribution is the one obtained by Rice and Johnson [11] and is proportional to δ/r, where δ is the crack opening displacement. Second, the condition that the plastic strain reaches the critical value ε_f^* at $r = \ell^*$ defines then the critical crack opening displacement δ_c. The latter is finally related to the fracture toughness by

$$\delta_c = 0.6\, K_{Ic}^2/E\sigma_Y \quad . \quad (8)$$

Hence,

$$K_{IC} = \text{const.}\ [\varepsilon_f^* \ell^* \sigma_Y E]^{1/2} \quad (9)$$

which is reminiscent of Eq. (1) in the HR-model. Although Ritchie et al. [9] advocate a sophisticated approach to obtain appropriate values for ε_f^* and ℓ^*, they conclude from their analysis of the upper shelf fracture toughness of irradiated pressure vessel steels that both ε_f^* and ℓ^* appear to decrease with increasing dose. The two parameters are therefore not basic materials parameters, but sensitive functions of the microstructure or the radiation hardening. This conclusion is then compatible with the meaning of the corresponding parameters in both the HR and the K model.

3. FLOW LOCALIZATION AND CHANNEL FRACTURE

In all fracture models discussed so far it was assumed that the plastic deformation around the crack tip is a continuous function. This basic assumption becomes invalid in high-strength materials, including those which attained their strength by radiation hardening. When these materials are plastically deformed even in a simple tensile test under uniform stress, plastic strain is observed to be highly localized within narrow deformation bands. In an extreme case, shown in Fig. 4 for irradiated type 304 stainless steel, the deformation channels are as narrow as 0.1 μm [12,13]. The macroscopically measured plastic strain at fracture is no longer an adequate measure for the much larger shear strain in the deformation channel. Therefore, the macroscopic fracture and ultimate tensile strain no longer have any meaning with regard to the localized deformation at a crack tip. Hence, different fracture models need to be developed when plastic flow is localized.

Before discussing the ingredients of such a model it is appropriate to review the conditions for localized flow in irradiated materials.

The sweeping-up of small dislocation loops by gliding dislocations appears to be the controlling factor in metals irradiated at low temperatures and to low doses. Channel deformation, as shown in Fig. 4, is exhibited by materials irradiated to high doses and at temperatures where swelling occurs. However, it is not clear whether the voids are instrumental or only conspicuous indicators in the flow localization process. In a recent analysis of this problem, the change in total energy, consisting of strain energy and surface energy, was found to increase as the voids are sheared. Although the strain energy of the voids decreases as they are sheared, the accompanying increase in surface energy is always larger for void sizes typical of irradiated materials. We conclude from this analysis that void formation is not solely responsible for channel deformation.

3.1 The Mori-Mura (MM) Model of Flow Localization

Dispersion-hardened alloys containing small dislocation loops have been considered by Mori and Mura [14] as a particular case of a material

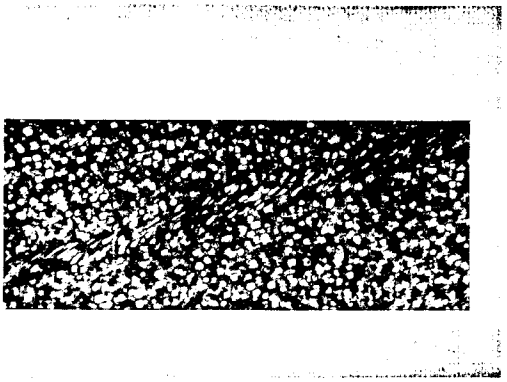

Fig. 4. Channel deformation in SA 304L.

with flow localization. It is assumed that the spherical precipitate particles deform only elastically in a plastic matrix, and that their backstress provides the source of the work-hardening. On the other hand, the dislocation loops in the matrix are eliminated whenever the local plastic shear exceeds a critical value γ_c. The strain energy of the eliminated loops represents an energy release mechanism leading to work softening. If γ is the plastic shear strain, and V_p the fractional volume occupied by deformation channels, so that $\bar{\gamma} = \gamma V_p$ is the macroscopic or average shear strain, then flow localization occurs whenever γV_p is bounded within the interval

$$\gamma_c - \frac{2E_\ell N_\ell}{\gamma_c f(1 - f)\,\mu A} \leq \gamma V_p \leq \gamma_c \quad . \tag{10}$$

Here, E_ℓ is the energy of a dislocation loop, N_ℓ the loop density, f the volume fraction occupied by the precipitate particles, and

$$A = \frac{(7 - 5\nu)}{2(4 - 5\nu) + \beta(7 - 5\nu)} \quad , \tag{11}$$

where ν is the Poisson's ratio of the matrix material, and $\beta = \mu/\mu'$ is the ratio of the shear modulii of the matrix and the precipitate, respectively. For a given value of the composite parameter $2E_\ell N_\ell/[f(1 - f)\mu A)]$ the two sides of the inequality (10) give lines shown in Fig. 5 which define the boundaries for regions of homogeneous deformation and localized flow. Assume, for example, that the critical shear for eliminating loops is $\gamma_c = 1\%$, and that the composite parameter is 5×10^{-4}. As the mean shear $\bar{\gamma} = \gamma V_p$ imposed onto the sample increases from zero to values larger than 1%, the deformation mode begins at first to be homogeneous, then becomes localized between about 0.5% and 1% mean shear, and reverses to the homogeneous mode thereafter. When the composite parameter becomes equal to 10^{-4} or larger, flow localization will occur no matter how small the macroscopic mean shear strain is. For a given γ_c, the plastic instability associated with immediate localized flow is reached when the loop density satisfies the relation

$$N_\ell > \frac{\mu A}{2E_\ell}\gamma_c^2 f(1 - f) = N_\ell^{crit} \quad . \tag{12}$$

The MM model for the onset of localized flow neglects perhaps many other important processes for work hardening and work softening in irradiated steels, but it clearly demonstrates that there are microstructural causes for flow localization and loss of ductility which can be identified and perhaps avoided.

3.2 The Fracture Model of Smith, Cook, and Rau (SCR)

Smith et al. [15] have developed a qualitative model for the fracture toughness of materials exhibiting flow localization. As a point of departure, they use the modified Griffith fracture criterion, and write

$$K_{Ic}^2 = E\Gamma_p/(1 - \nu^2) \quad . \tag{13}$$

Γ_p is the "plastic surface energy", and it replaces the actual surface energy appropriate for truly brittle solids. If $\tau(\gamma)$ is the shear stress in a deformation band emanating from the crack tip, then

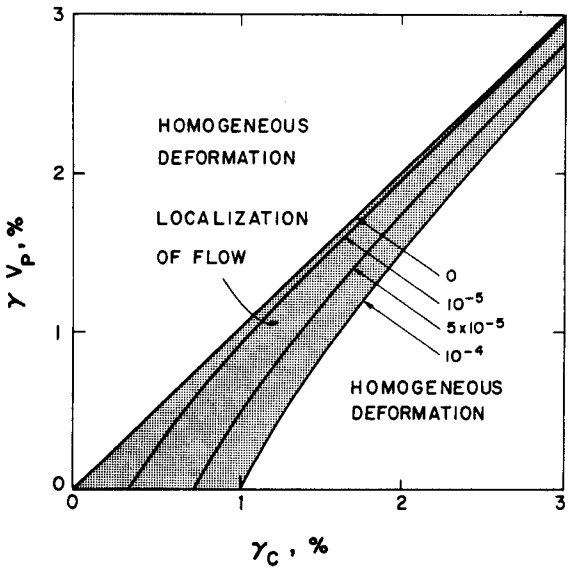

Fig. 5. Conditions for flow localization in the Mori-Mura model. Numbers designating the various curves are for the composite parameter $2E_\ell N_\ell/[f(1 - f)\mu A]$.

$$\Gamma_p = b \int_0^{\gamma_f} \tau(\gamma)\, d\gamma \qquad (14)$$

where b is the Burgers vector.

After a certain amount of shear has taken place, decohesion will occur when $\gamma = \gamma_f$, at which point $\tau(\gamma_f) = 0$. Although $\tau(\gamma)$ is not known, one can assume that $\tau(\gamma)$ is of the order of σ_γ for $\gamma < \gamma_f$, and write

$$\Gamma_p = \sigma_\gamma w_f \qquad (15)$$

where w_f is the critical shear displacement for glide decohesion. In a sense, it replaces the critical COD δ_c in ductile fracture models. With Eq. (15), Smith et al. [15] obtain finally the relationship

$$K_{Ic} = \phi \sqrt{E \sigma_\gamma w_f} \qquad (16)$$

for the fracture toughness, where $\phi(\alpha)$ is a numerical factor which depends on the inclination angle α of the deformation band to the crack plane.

3.3 Application of the SCR-Model to Channel Fracture

The angular function $\phi(\alpha)$ is not specified in the SCR-model. However, Vitek [16] has analyzed the problem of inclined glide planes emanating from a crack tip according to the Bilby-Cottrell-Swinden crack model. We can combine Vitek's result with the SCR-model and obtain

$$K_{Ic} \cong \frac{3.58}{\sin\alpha \cos\alpha} \sqrt{\frac{\mu \tau_o w_f}{\sin\alpha}} \qquad (17)$$

where τ_o is the resolved shear stress for dislocation glide. For given values of the parameters μ, τ_o, and w_f, the lowest value for K_{Ic} is obtained when the glide planes are inclined to the crack plane at an angle α_m given by $\cos\alpha_m = \sqrt{2/5}$ or $\alpha_m \cong 50.8°$. Hence

$$K_{Ic} \cong 8.3 \sqrt{\mu \tau_o w_f} \quad . \qquad (18)$$

A further modification of this equation is required when the glide bands emanating from the crack tip contain not one but N parallel glide planes contained within a channel of width d, so that Nb = d. Then

$$K_{Ic} \cong 8.3 \sqrt{\mu \tau_o w_f} = 8.3 \sqrt{\mu \tau_o d (w_f/b)} \quad . \qquad (19)$$

A line originally perpendicular to the glide planes will, after shearing of the channel, rotate through an angle ψ given by $\tan\psi = w/b$. Hence, the critical decohesion displacement w_f corresponds to a critical shear angle ψ_f, and we can write

$$K_{Ic} \cong 8.3 \sqrt{\mu \tau_o d (\tan\psi_f)} \quad . \qquad (20)$$

We can now apply this relationship to channel fracture. Assuming that the deformation channel shown in Fig. 4 is typical of those formed at a crack tip, we find by inspection of the sheared voids that the critical shear angle must satisfy

$$\tan\psi_f \gtrsim 2$$

since no decohesion can be seen in this channel. Assuming $\tau_o/\mu = 10^{-2}$ and d = 0.15 μm, we find that for the irradiated material shown in Fig. 4

$$K_{Ic} \gtrsim 30 \text{ MPa } \sqrt{m} \quad .$$

This lower-bound estimate represents still a very respectable fracture toughness for a thin-walled structure in spite of the very low ductility exhibited by this material.

The present analysis demonstrates then that even though flow localization in highly irradiated materials leads to extreme brittleness in terms of uniaxial fracture strains, a satisfactory fracture toughness may still be retained.

4. RADIATION EFFECTS ON FATIGUE CRACK GROWTH

Fatigue crack growth rates, when plotted as a function of the cyclic stress concentration ΔK, exhibit three stages indicated in Fig. 6. In the intermediate Stage II, crack growth is often described by the Paris law

$$da/dN = C(\Delta K)^m \qquad (21)$$

where C and m are materials parameters. The terminal Stage III of fatigue crack growth is limited by the static fracture toughness K_{Ic}. With increasing radiation damage, K_{Ic} drops, and one expects that Stage II is narrowed or shifted to lower values of ΔK. Furthermore, it has been found [17] that the crack growth exponent m and the static fracture toughness K_{Ic} are related. Figure 7 shows this empirical relationship with the various data points for medium and high strength steels deleted. It can be seen that the crack growth rate becomes extremely sensitive to ΔK whenever the static fracture toughness drops below 50 MPa $\sqrt{m}$. According to the K-model predictions for K_{Ic} as shown in Fig. 3, radiation effects will not affect the fatigue crack growth exponent below a dose of 10 dpa. This is in agreement with the experimental findings of James [18,19] on both irradiated austenitic [18] as well as ferritic [19] steels. Little or no effect of fast reactor irradiations was found on the fatigue crack growth rate for doses of 4 dpa or less and irradiation and test temperatures below 500°C. Nevertheless, based on the expected further reduction of K_{Ic} with dose, one must expect an effect on the Stage II fatigue crack growth at doses above perhaps 15 dpa. This reduction in K_{Ic} with the potential acceleration of fatigue crack growth is an important life-limiting factor for the first wall of a tokamak reactor, as has been demonstrated by Watson et al. [1].

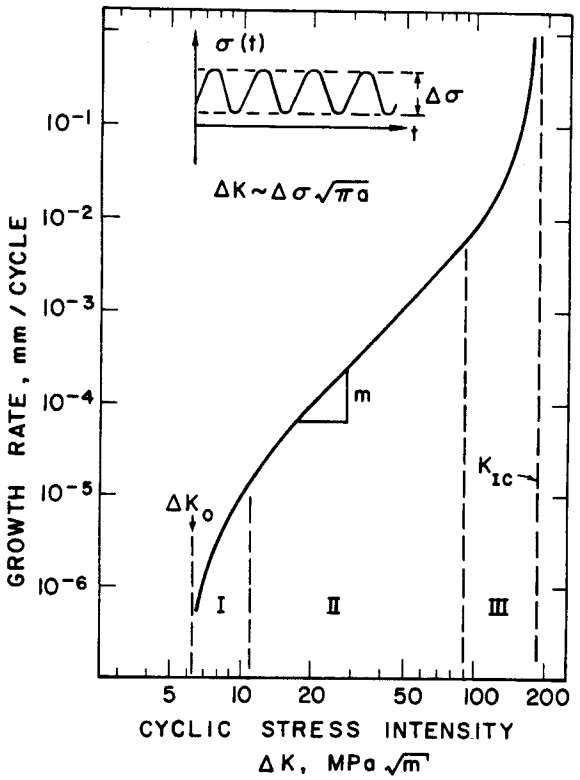

Fig. 6. Typical fatigue crack growth curve.

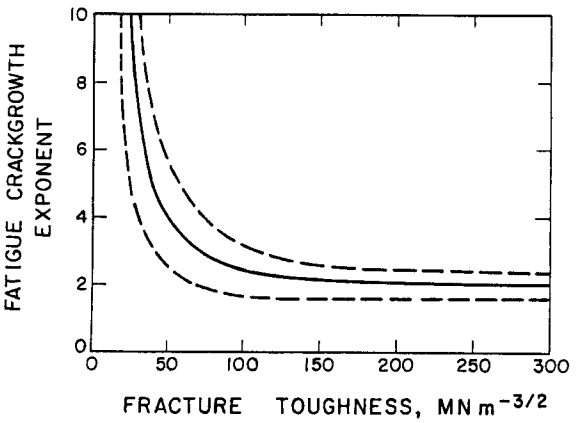

Fig. 7. Variation of the fatigue crack growth exponent m with fracture toughness.

Stage I of fatigue crack growth, where the growth rate da/dn $\lesssim 10^{-6}$ cm/cycle, and the magnitude of the threshold ΔK_0, are of particular importance for a long lifetime of the first wall. Unfortunately, experimental measurements of Stage I fatigue crack growth on irradiated materials are virtually absent. Accordingly, one has to rely on the general observation and experience that the threshold ΔK_0 is sensitive to the chemical environment, to the R-ratio ($R = K_{max}/K_{min}$, where K_{max} and K_{min} are the maximum and minimum stress concentration factors obtained for the cyclic loading), to the impurity segregation at grain boundaries, and to the susceptibility of high-strength materials to flow localization. The latter observation is related to the empirical correlation [20-22], shown in Fig. 8, that the threshold ΔK_0 decreases with yield strength particularly for high-strength steels. Based on this correlation, excessive radiation hardening is expected to lead to a similar reduction in the threshold ΔK_0 and to an increase in fatigue crack growth in Stage I, the most important range of fatigue crack growth for first wall applications to tokamak reactors.

5. MODELING CHEMICAL ENVIRONMENT EFFECTS ON FATIGUE AND FRACTURE

Design studies of tokamak reactors and detailed modeling of the failure modes of first walls have shown that under normal operating conditions, the fatigue crack growth of flaws on the coolant side of the first wall leads to shorter lifetimes than flaws on the plasma side [1]. As a result, corrosion effects by the coolant in conjunction with radiation damage and hydrogen and helium embrittlement are of great concern.

Stress corrosion and corrosion fatigue models have emphasized dissolution controlled crack growth processes for both intergranular and transgranular fracture where the major contribution of crack tip stresses and strains is to fracture the corrosion limiting passive film. In these models, crack growth rates depend on film rupture, repassivation and anodic dissolution rates. There is little disagreement that intergranular stress corrosion cracking of sensitized stainless steel is a dissolution rate controlled process; however, the picture is not as clear for transgranular stress corrosion and corrosion fatigue. Evidence of cleavage-like fracture surfaces has been shown for austenitic stainless steels [23], ferritic steels [24] and brasses [25] tested in corrosive environments. In ferritic steels, hydrogen embrittlement is clearly implicated, but in austenitic stainless steels and brasses hydrogen embrittlement has not been identified as the cause of the cleavage like fracture surfaces. Therefore, a physical process other than hydrogen or dissolution must be considered to explain these fracture surfaces. Some possible processes include corrosion generated di-vacancy hardening or enhanced creep, corrosion modified crack tip flow properties, or surface adsorption/energy effects on fracture.

The effect of a corrosive environment on fracture or fatigue can also be expressed with

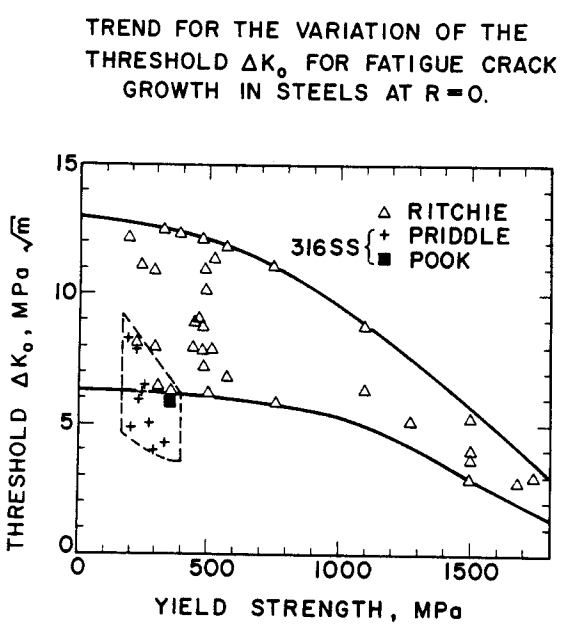

Fig. 8. Threshold for fatigue crack growth versus yield strength.

fracture models by Hahn and Rosenfield [2], Eq. (1), or fatigue models by McClintock [26], Eq. (22), or Broek and Rice [27], Eq. (23). These models relate K_{Ic} and da/dN to material parameters as follows:

$$da/dN \sim \Delta K^2/2\sigma_Y E \qquad (22)$$

$$da/dN = \frac{(\Delta K - \Delta K_o)^2 \, C\Delta K^m}{(1 - R) K_{Ic} - \Delta K} \quad . \qquad (23)$$

Use of Eq. (1) to evaluate the effect of a corrosion environment on subcritical flaws is not a direct measure of K_{Iscc}, since K_{Ic} is the stress intensity for critical flaw growth. However, if ε^* and σ_Y are defined as local properties of the material within a few μm of the crack tip, then K_{Ic} in Eq. (1) can be defined as the local fracture toughness, K'_{Ic}. A corrosive environment could reduce K'_{Ic} by changes in ε^*, ℓ, or σ_Y. Hydrogen uptake could decrease ε^* by a variety of embrittlement processes and increase or decrease σ_Y and ℓ by hardening or softening processes. Corrosion has been observed to reduce ε^* during slow strain rate tests of materials and this data can be used to assess the effect of corrosion on K'_{Ic}. For instance, Mom et al. [28] observed a strain to failure of 1.5% for 304 SS tested at 123°C in 35% $MgCl_2$ as compared to a strain to failure of 50% in air. Assuming that the corrosive environment altered only ε^* in Eq. (1), the ratio between K'_{Ic} in $MgCl_2$ to that in air is

$$\frac{K'_{Ic}}{K_{Ic}} = \sqrt{\frac{\varepsilon^*(MgCl_2)}{\varepsilon^*(air)}} \approx 0.173 \quad .$$

If K_{Ic} in air is 100 MPa $\sqrt{m}$, then K'_{Ic} is 17 MPa $\sqrt{m}$. This value is an upper bound on K_{Iscc} since K_{Iscc} must be less than or equal to K'_{Ic}. This calculation is only an example, and unfortunately experimental values for K_{Iscc} in $MgCl_2$ are not readily available. An effort to evaluate Eqs. (1), (22), (23) would require performing constant extension rate tests, pre-cracked fracture tests and fatigue tests with the materials and environments of interest.

The yield stress of materials tested in corrosive environments can also be altered in comparison with those measured in inert environments. This effect has been most clearly demonstrated by Kramer and Demer [29] on aluminum monocrystals which showed a decreased yield strength after a strain-electropolish cycle. A time dependent elongation was observed during anodic dissolution of copper [30] and stainless steel [31] which were loaded to 150 to 200% of their yield strengths. Therefore, the flow stress in the region of the crack tip can be expected to decrease as a result of crack tip dissolution. Anodic dissolution may occur as a result of film rupture or in cases when a passive film may not be stable. A decrease in the crack tip flow stress would decrease K'_{Ic} (Eq. 1) while increasing da/dN (Eqs. 22 and 23). Therefore, stress corrosion cracking and corrosion fatigue can be related to changes in ε_f and σ_Y. Both of these parameters can be measured with simple slow strain rate tests, but the tests must be conducted at relevant electrochemical potentials, pH's, chemical compositions (O_2, Cl, etc.) and with a notched tensile sample.

6. FRACTURE DESIGN CRITERIA

Safety considerations may make it desirable to design the first wall such that the ultimate failure may not be catastrophic in the sense that a very large crack develops suddenly and much coolant is spilled into the plasma chamber. To mitigate against such a failure mode, it may be prudent to require two failure criteria:

A) through-thickness yielding before break;

B) and leak before break.

The criterion A defines for a given fracture toughness K_{Ic} and given yield stress σ_Y a wall thickness

$$h \leq (K_{Ic}/\sigma_Y)^2 \qquad (24)$$

for which failure will occur by through-the-thickness yielding before a crack would propagate catastrophically. This condition derives

from the fact that $(K_{Ic}/\sigma_Y)^2$ is of the order of the plastic zone dimension at the crack tip. When this plastic zone is equal to or larger than the wall thickness a state of plane stress exists in the plastic zone rather than a state of plane strain, and the crack extends by ductile tearing before propagating catastrophically.

To further illustrate the meaning of this failure criterion, we consider a first wall made of 20% CW type 316 stainless steel and operated at a temperature of 420°C. The yield strength changes as a function of the displacement damage according to the correlation by Simons [32], whereas the change of fracture toughness is based on the model predictions in sections 2 and 3. Using these results shown in Fig. 9, the "safe" wall thickness can be evaluated according to $h_s = (K_{Ic}/\sigma_Y)^2$. The result is shown in Fig. 10. For wall thicknesses below h_s, yielding occurs before break, whereas break takes place before yielding when $h > h_s$. Conversely, a wall thickness of 0.5 cm would no longer be safe in the spirit of the fracture design criterion A after an irradiation dose of 25 dpa.

It must be emphasized that the criterion A may be too conservative when the applied loads produce a total tensile stress much below the yield stress. In this case, the criterion B of "leak before break" is more appropriate. It was proposed by Irwin [33], and it states that the critical crack size for a given design stress level σ should be larger than the wall thickness h. This implies that any part-through crack remains below critical. This condition is expressed by the relationship

$$\left(\frac{K_{Ic}^2}{\sigma_Y^2 h}\right)\left[1 + 1.4\left(\frac{K_{Ic}^2}{\sigma_Y^2 h}\right)^3\right] \geq \frac{\pi(\sigma/\sigma_Y)^2}{1 - (\sigma/\sigma_Y)^2/2} \quad . \qquad (25)$$

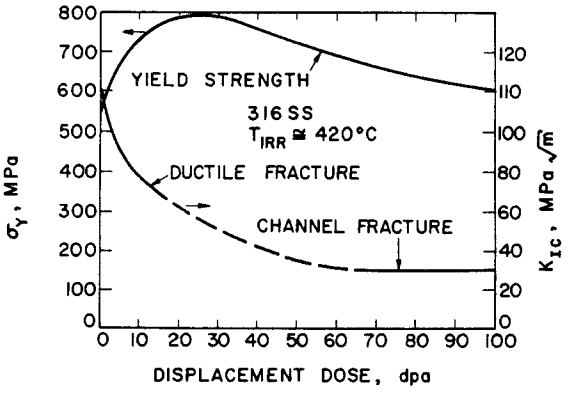

Fig. 9. Measured yield strength variation for EBR-II irradiated 316 SS and estimated fracture toughness versus displacement dose.

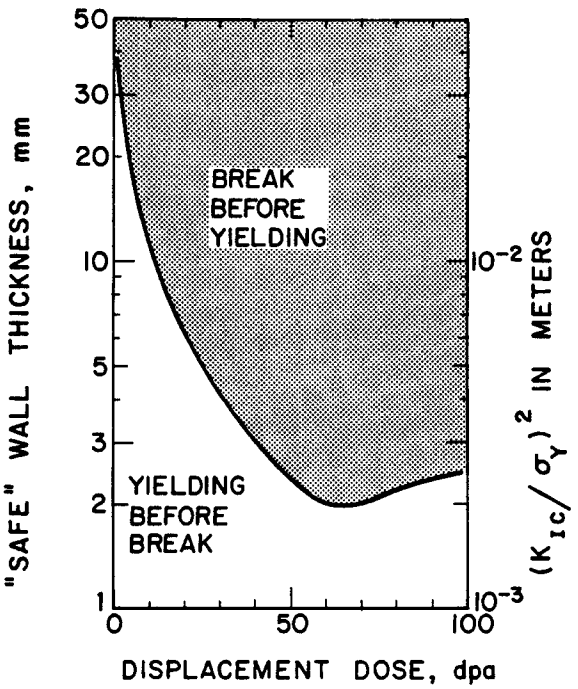

Fig. 10. Estimated wall thicknesses satisfying the yield-before-break failure criterion.

The minimum value of $K_{Ic}/\sigma_Y \sqrt{h}$ which satisfies this criterion B is plotted in Fig. 11 as a function of σ/σ_Y. It is seen that criterion B is more conservative than criterion A when $\sigma \lesssim 3\sigma_Y/4$. For conditions covered by the cross-hatched area in Fig. 11, where criterion B is less conservative than A, a part-through crack will first propagate by ductile tearing when $K_{Ic}/\sigma_Y \sqrt{h}$ is larger than one.

The implementation of the two proposed fracture design criteria will require that the critical materials parameter K_{Ic} and σ_Y are known as a function of irradiation dose and temperature. The first wall will have to be exchanged at the time when either of the two criteria is violated even though no failure may have occurred yet. Failure prior to this time will take the form of coolant leaks; failure after this time may produce large ruptures and extensive coolant spills.

ACKNOWLEDGMENTS

This work was supported by the U.S. Department of Energy under contract ER-78-S-02-4861 with the University of Wisconsin and under contract DE-AC06-76RLO-1830 with the Battelle Memorial Institute.

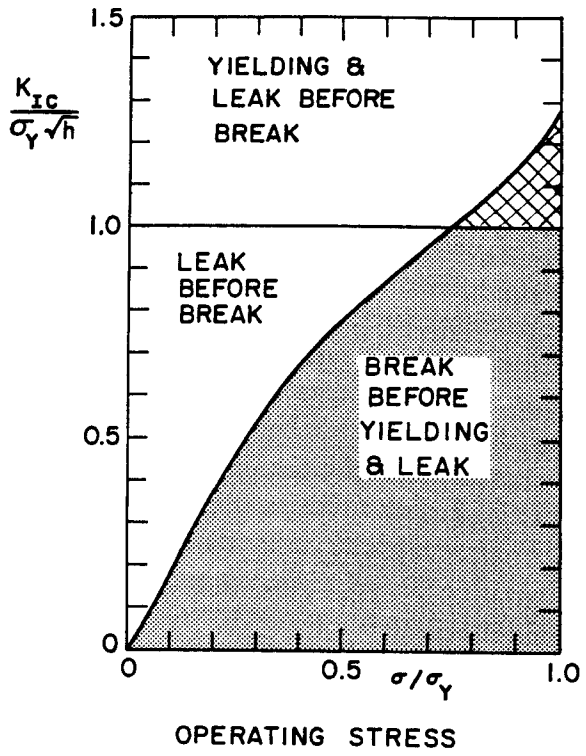

Fig. 11. Failure criteria diagram.

REFERENCES

[1] Watson, R.D., Peterson, R.R., and Wolfer, W.G.; these proceedings.

[2] Hahn, G.T. and Rosenfield, A.R.; in Applications related phenomena in titanium alloys, ASTM STP 432 (1968) 5.

[3] Bilby, B.A. and Swinden, K.H.; Proc. Roy. Soc. London A285 (1965) 22.

[4] Grossbeck, M.L. and Maziasz, P.J.; J. Nucl. Matls. 85 & 86 (1979) 883.

[5] Dufresne, J., Henry, B., and Larsson, H.; in Effects of radiation on structural materials, ASTM STP 683 (1979) 511.

[6] Krafft, J.M.; Appl. Matls. Res. 3 (1964) 88.

[7] Ritchie, R.O., Knott, J.F., and Rice, J.R.; J. Mech Phys. Solids 21 (1973) 395.

[8] Parks, D.M.; Trans. ASME, J. Eng. Matls. and Techn. 98 (1976) 30.

[9] Ritchie, R.O., Server, W.L., and Wullaert, R.A.; Met. Trans. A10 (1979) 1557.

[10] Rice, J.R.; in Fracture, Vol. 2, Ch. 3; ed. H. Liebowitz, Acad. Press, NY (1968).

[11] Rice, J.R. and Johnson, M.A.; in Inelastic behavior of solids, ed. M.F. Kanninen et al., McGraw Hill, NY, (1970) 641.

[12] Flinn, J.E., Krajcinovic, D., Phipps, R.D., Franklin, D.G., and Miller, S.C.; Report ANL/EBR-068, Feb. 1973.

[13] Fish, R.L., Straalsund, J.L., Hunter, C.W., and Holmes, J.J.; in Effects of rad. on substructure and mech. properties of metals and alloys, ASTM STP 529 (1973) 149.

[14] Mori, T. and Mura, T.; Matls. Science and Eng. 26 (1976) 89.

[15] Smith, E., Cook, T.S., and Rau, C.A.; Fracture 1977, Vol. 1, ICF4, Waterloo, Canada, 215.

[16] Vitek, V.; J. Mech. Phys. Solids 24 (1976) 263.

[17] Ritchie, R.O. and Knott, J.F.; Acta Met. 21 (1973) 639.

[18] James, L.A.; J. Nucl. Matls. 59 (1976) 183.

[19] James, L.A.; Trans. ASME, J. Eng. Matls. Techn. 102 (1980) 187.

[20] Ritchie, R.O.; Metal Science 11 (1977) 368.

[21] Priddle, E.K., Walker, F., and Wiltshire, C.; Paper C115, Joint I. Mech. E. and Soc. Environmental Engrs. Conf., London, May 1977.

[22] Pook, L.P.; in Proc. 1971 Nat. Symp. on Fracture Mech., Part 1, ASTM STP 513 (1972), 106.

[23] Liu, R., Nanita, N., Alstetter, C., Birnbaum, H., and Pugh, E.N.; Met. Trans. 11A (1980) 1563.

[24] Scully, J.C.; Stress corrosion cracking and hydrogen embrittlement of iron base alloys, R.W. Staehle, J. Hochmann, R.D. McCright, and J.E. Slater, eds., NACE-5 (1973) 946.

[25] Beavers, J.A. and Pugh, E.N.; Met. Trans. 11A (1980) 809.

[26] McClintock, F.A.; Fatigue crack propagation, STP-415, Philadelpha, PA (1967) 170.

[27] Broek, D. and Rice, R.C.; Materials and processes in service performance, (1977) 392.

[28] Mom, A.J.A., Dencher, R.T., Wekken, C.J.V.D., and Schultze, W.A.; Stress corrosion cracking -- the slow strain rate technique, G.M. Vgianski and J.H. Payer, eds. ASTM STP-665 (1979) 305.

[29] Kramer, I.R. and Demer, L.J.; Trans. AIME 221 (1961) 780.

[30] Revie, R.W. and Uhlig, H.H.; Acta Met. 22 (1974) 619.

[31] Smialowski, M. and Kostanski, M.; Corrosion Sci. 19 (1979) 1019.

[32] Simons, R.L.; these proceedings.

[33] G.R. Irwin; Trans. ASME, Series A 86 (1964) 444.